

The five-gluon amplitude in the high-energy limit

This article has been downloaded from IOPscience. Please scroll down to see the full text article.

JHEP12(2009)023

(<http://iopscience.iop.org/1126-6708/2009/12/023>)

[The Table of Contents](#) and [more related content](#) is available

Download details:

IP Address: 80.92.225.132

The article was downloaded on 01/04/2010 at 13:20

Please note that [terms and conditions apply](#).

The five-gluon amplitude in the high-energy limit

Vittorio Del Duca,^a Claude Duhr^b and E.W. Nigel Glover^c

^a*Istituto Nazionale di Fisica Nucleare, Laboratori Nazionali di Frascati,
00044 Frascati, Roma, Italy*

^b*Institut de Physique Théorique & Centre for Particle Physics and Phenomenology (CP3),
Université Catholique de Louvain,
Chemin du Cyclotron 2, B-1348 Louvain-la-Neuve, Belgium*

^c*Institute for Particle Physics Phenomenology, University of Durham
Durham, DH1 3LE, U.K.*

E-mail: delduca@lnf.infn.it, claudе.duhr@uclouvain.be,
e.w.n.glover@durham.ac.uk

ABSTRACT: We consider the high-energy limit of the colour-ordered one-loop five-gluon amplitude in the planar maximally supersymmetric $\mathcal{N} = 4$ Yang-Mills theory in multi-Regge kinematics where all of the gluons are strongly ordered in rapidity. We apply the calculation of the one-loop pentagon in $D = 6 - 2\epsilon$ performed in a companion paper [1] to compute the one-loop five-gluon amplitude through to $\mathcal{O}(\epsilon^2)$. Using the factorisation properties of the amplitude in the high-energy limit, we extract the one-loop gluon-production vertex to the same accuracy, and, by exploiting the iterative structure of the gluon-production vertex implied by the BDS ansatz, we perform the first computation of the two-loop gluon-production vertex up to and including finite terms.

KEYWORDS: Supersymmetric gauge theory, Gauge Symmetry, QCD

ARXIV EPRINT: [0905.0100](https://arxiv.org/abs/0905.0100)

Contents

1	Introduction	1
2	Five-point amplitudes in multi-Regge kinematics	2
2.1	Tree amplitudes in multi-Regge kinematics	3
2.2	High-energy factorisation of the five-point amplitude	4
2.3	The two-loop five-point amplitude and the BDS ansatz	7
2.4	Analytic continuation of the five-point amplitude to the physical region	8
3	The one-loop five-point amplitude	9
3.1	Soft limit	11
4	The one-loop gluon-production vertex	12
4.1	Analytic continuation of the one-loop vertex to the physical region	13
5	The two-loop gluon-production vertex	16
6	Conclusions	17
A	Multi-parton kinematics	18
B	Multi-Regge kinematics	20
C	The soft limit of the one-loop five-point amplitude	20

1 Introduction

The colour-stripped one-loop five-gluon MHV amplitude in the planar maximally supersymmetric $\mathcal{N} = 4$ Yang-Mills theory to all orders in ϵ is given by [2, 3],

$$m_5^{(1)}(1, 2, 3, 4, 5) = -\frac{1}{4} \sum_{\text{cyclic}} s_{12}s_{23} I_4^{1m}(1, 2, 3, 45, \epsilon) - \frac{\epsilon}{2} \epsilon_{1234} I_5^{6-2\epsilon}(\epsilon), \quad (1.1)$$

where $m_5^{(1)}$ denotes the one-loop coefficient, i.e., the one-loop amplitude rescaled by the tree-level amplitude, and where the cyclicity is over $i = 1, \dots, 5$. Here $I_4^{1m}(1, 2, 3, 45, \epsilon)$ represents the one-mass box integral with an off-shell leg of virtuality s_{45} , $I_5^{6-2\epsilon}(\epsilon)$ is the (massless) one-loop pentagon integral evaluated in $6 - 2\epsilon$ dimensions, and the contracted Levi-Civita tensor is $\epsilon_{1234} = \text{tr}[\gamma_5 \not{k}_1 \not{k}_2 \not{k}_3 \not{k}_4]$. In a companion paper [1], we have performed the first analytic computation of the higher dimension pentagon, $I_5^{6-2\epsilon}(\epsilon)$, albeit in the simplified case of *multi-Regge kinematics* [4]. In this limit, we have derived $I_5^{6-2\epsilon}(\epsilon)$ as an all-order expression in ϵ , and explicitly expanded it through to $\mathcal{O}(\epsilon^2)$.

In the high-energy limit (HEL) $s \gg |t|$, any scattering process is dominated by the exchange of the highest-spin particle in the crossed channel. Thus, in perturbative QCD the leading contribution in powers of s/t to any scattering process comes from gluon exchange in the t channel. In this limit, scattering amplitudes undergo a Regge factorisation [4, 5] which allows an amplitude for gluon exchange to be decomposed in terms of building blocks associated with the various components of the amplitude. In the simplest case of four-gluon scattering, one exchanges a reggeised gluon (representing a gluon ladder) that is emitted from one scattering vertex and absorbed at the other. This emission is described by the coefficient function or impact factor. For processes involving more gluons, additional gluons are emitted by the gluon ladder and this emission is controlled by the gluon-production (or Lipatov) vertex. Using the high-energy factorisation for colour-stripped amplitudes [6, 7], we can relate the one-loop gluon-production vertex in the $\mathcal{N} = 4$ super Yang-Mills theory to the one-loop five-gluon amplitude given in eq. (1.1) and extract it through to $\mathcal{O}(\epsilon^2)$.

Recently, Bern, Dixon and Smirnov (BDS) have proposed an iterative ansatz [8, 9] for the l -loop n -gluon scattering amplitude in the maximally supersymmetric $\mathcal{N} = 4$ Yang-Mills theory (MSYM), with the maximally-helicity violating (MHV) configuration and for arbitrary l and n . The iterative structure of the BDS ansatz has been shown to be correct for the two-loop five-point amplitude through direct numerical calculation [3]. Together with the high-energy factorisation, that implies an iterative structure of the gluon-production vertex [7]. Thus, the knowledge of the one-loop gluon-production vertex through to $\mathcal{O}(\epsilon^2)$, allows us to perform the first computation of the two-loop gluon-production vertex up to and including the finite terms.

Our paper is organised as follows. In section 2 we consider the five-point amplitude in multi-Regge kinematics. First we make a precise definition of multi-Regge kinematics and review how the tree-level MHV amplitude factorises in the high energy limit. The factorisation properties of the five-gluon amplitude are described in section 2.2 and the relationship between the one-loop amplitude and the one-loop Lipatov vertex established. We remind the reader of the iterative structure of the Lipatov vertex in section 2.3 while its analytic continuation properties are discussed in section 2.4. In section 3 we present the one-loop five-point amplitude through to $\mathcal{O}(\epsilon^2)$ and use it to compute the one-loop gluon-production vertex through to $\mathcal{O}(\epsilon^2)$ in section 4 where we find contributions from both the parity-even and parity-odd parts. In section 5 we compute the two-loop gluon-production vertex through to finite terms. Our findings are briefly summarised in section 6. Some of the technical details are enclosed in the appendices. Further details on the multi-parton light-cone momenta and how they behave in multi-Regge kinematics are given in appendices A and B, while the soft limit of the one-loop Lipatov vertex is further discussed in appendix C.

2 Five-point amplitudes in multi-Regge kinematics

We consider a five-point amplitude, $g_1 g_2 \rightarrow g_3 g_4 g_5$, with all the momenta taken as outgoing, and label the legs cyclically clockwise. In multi-Regge kinematics [4], the produced particles are strongly ordered in rapidity and have comparable transverse momenta,

$$y_3 \gg y_4 \gg y_5; \quad |p_{3\perp}| \simeq |p_{4\perp}| \simeq |p_{5\perp}|. \quad (2.1)$$

Accordingly, the Mandelstam invariants can be written in the approximate form (B.3).¹ We label the momenta transferred in the t -channel as

$$q_1 = p_1 + p_5, \quad q_2 = -p_2 - p_3, \quad (2.2)$$

with virtualities $t_i = q_i^2$. Then it is easy to see that in multi-Regge kinematics the transverse components of the momenta q_i dominate over the longitudinal components, $q_i^2 \simeq -|q_{i\perp}|^2$. In addition, $t_1 = s_{15}$ and $t_2 = s_{23}$, and we label $s = s_{12}$, and $s_1 = s_{45}$, $s_2 = s_{34}$. Thus, eq. (2.1) becomes

$$s \gg s_1, \quad s_2 \gg -t_1, \quad -t_2. \quad (2.3)$$

Labelling the transverse momentum of the particle emitted along the ladder as $\kappa = |p_{4\perp}|^2$, we can write

$$\kappa = \frac{s_1 s_2}{s}, \quad (2.4)$$

which is known as the mass-shell condition (B.4).

2.1 Tree amplitudes in multi-Regge kinematics

The colour decomposition of the tree-level five-point amplitude is [10]

$$\mathcal{M}_5^{(0)}(1, 2, 3, 4, 5) = 2^{5/2} \sum_{S_5/Z_5} \text{tr} \left(T^{d_1} \dots T^{d_5} \right) m_5^{(0)}(1, 2, 3, 4, 5), \quad (2.5)$$

where d_i is the colour of a gluon of momentum p_i and helicity ν_i . The T 's are the colour matrices² in the fundamental representation of $SU(N)$ and the sum is over the noncyclic permutations S_5/Z_5 of the set $[1, \dots, 5]$. For five gluons, there are only MHV helicity configurations $(-, -, +, +, +)$ for which the tree-level gauge-invariant colour-stripped amplitudes assume the form

$$m_5^{(0)}(1, 2, 3, 4, 5) = g^3 \frac{\langle p_i p_j \rangle^4}{\langle p_1 p_2 \rangle \langle p_2 p_3 \rangle \langle p_3 p_4 \rangle \langle p_4 p_5 \rangle \langle p_5 p_1 \rangle}, \quad (2.6)$$

where i and j are the two gluons of negative helicity. The colour structure of eq. (2.5) in multi-Regge kinematics is known [11–13] and will not be considered further. Here we concentrate on the behaviour of the colour-stripped amplitude (2.6). Using the spinor products in multi-Regge kinematics (B.5), the amplitude (2.6) takes the factorised form [12],

$$m_5^{(0)}(1, 2, \dots, 5) = s \left[g C^{(0)}(p_2, p_3) \right] \frac{1}{t_2} \left[g V^{(0)}(q_2, q_1; \kappa) \right] \frac{1}{t_1} \left[g C^{(0)}(p_1, p_5) \right] \quad (2.7)$$

which is shown schematically in figure 1.

The gluon coefficient functions $C^{(0)}$, which yield the LO gluon impact factors, are given in ref. [4] in terms of their spin structure and in ref. [12, 14] at fixed helicities of the external gluons,

$$C^{(0)}(p_2^-, p_3^+) = 1 \quad C^{(0)}(p_1^-, p_5^+) = \frac{p_{5\perp}^*}{p_{5\perp}}, \quad (2.8)$$

¹A physically more intuitive representation of the invariants in terms of rapidities is given in ref. [7].

²We use the normalization $\text{tr}(T^c T^d) = \delta^{cd}/2$, although it is immaterial in what follows.

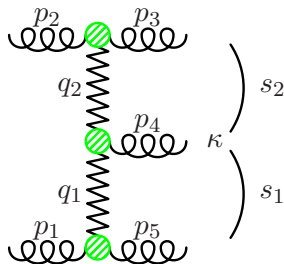


Figure 1. Five-point amplitude in multi-Regge kinematics. The green blobs indicate the coefficient functions (impact factors) and the vertex describing the emission of gluons along the ladder.

with the complex transverse momentum $p_{\perp} = p_x + ip_y$. The vertex for the emission of a gluon along the ladder is [12, 15, 16]

$$V^{(0)}(q_2, q_1, \kappa) = \sqrt{2} \frac{q_{2\perp}^* q_{1\perp}}{p_{4\perp}}, \quad (2.9)$$

with $p_4 = q_2 - q_1$.

2.2 High-energy factorisation of the five-point amplitude

The Regge factorisation of the tree-level colour-stripped amplitude is given by eq. (2.7). In the leading logarithmic (LL) approximation, the virtual radiative corrections to eq. (2.7) are obtained, to all orders in α_s , by replacing the propagator of the t -channel gluon by its reggeised form [4]. That is, by making the replacement

$$\frac{1}{t_i} \rightarrow \frac{1}{t_i} \left(\frac{s_i}{\tau} \right)^{\alpha(t_i)}, \quad (2.10)$$

in eq. (2.7), with $\alpha(t_i)$ related to the loop transverse-momentum integration

$$\alpha(t_i) = \alpha_s N_c t_i \int \frac{d^2 k_{\perp}}{(2\pi)^2} \frac{1}{k_{\perp}^2 (q_i - k)_{\perp}^2} + \mathcal{O}(\alpha_s^2) \quad t_i = q_i^2 \simeq -|q_{i\perp}|^2, \quad (2.11)$$

and $\alpha_s = g^2/4\pi$. The infrared divergence in eq. (2.11) can be regulated in 4 dimensions with an infrared-cutoff mass. Alternatively, using dimensional regularization in $d = 4 - 2\epsilon$ dimensions, the integral in eq. (2.11) is performed in $2 - 2\epsilon$ dimensions, yielding

$$\alpha(t_i) = g^2 c_{\Gamma} \left(\frac{\mu^2}{-t_i} \right)^{\epsilon} N \frac{2}{\epsilon} + \mathcal{O}(g^4), \quad (2.12)$$

with N colours, and

$$c_{\Gamma} = \frac{1}{(4\pi)^{2-\epsilon}} \frac{\Gamma(1+\epsilon) \Gamma^2(1-\epsilon)}{\Gamma(1-2\epsilon)}. \quad (2.13)$$

$\alpha(t_i)$ is the Regge trajectory and accounts for the higher-order corrections due to gluon exchange in the t_i channel. In eq. (2.10), the reggeisation scale τ is introduced to separate contributions to the reggeized propagator, the coefficient function and the gluon-production vertex. It is much smaller than any of the s -type invariants, and it is of the order of the t -type invariants. In order to go beyond the LL approximation and to compute

the higher-order corrections to the gluon-production vertex (2.9), we need a high-energy prescription [5] which disentangles the virtual corrections to the gluon-production vertex from those to the coefficient functions (2.8) and from those that reggeize the gluon (2.10). The high-energy prescription of ref. [5] is given at the colour-dressed amplitude level in QCD, where it holds to the next-to-leading-logarithmic (NLL) accuracy. In ref. [6], we showed that the high-energy prescription, when applied to the colour-stripped four-point amplitude, is valid up to three loops. In ref. [7], we conjectured the factorised form of a generic colour-stripped n -gluon amplitude in multi-Regge kinematics. For the five-point amplitude, $g_1 g_2 \rightarrow g_3 g_4 g_5$, that prescription yields

$$m_5 = s [g C(p_2, p_3, \tau)] \frac{1}{t_2} \left(\frac{-s_2}{\tau} \right)^{\alpha(t_2)} [g V(q_2, q_1, \kappa, \tau)] \frac{1}{t_1} \left(\frac{-s_1}{\tau} \right)^{\alpha(t_1)} [g C(p_1, p_5, \tau)] , \quad (2.14)$$

with the invariants labelled as in section 2, i.e., $t_1 = s_{51}$, $t_2 = s_{23}$, $s_1 = s_{45}$ and $s_2 = s_{34}$. In eq. (2.14), we suppressed the dependence of the coefficient function and of the gluon-production vertex on the dimensional regularisation parameters μ^2 and ϵ . In order for the amplitude m_5 to be real, eq. (2.14) is taken in the Euclidean region where all the invariants are negative,

$$s, s_1, s_2, t_1, t_2, \kappa < 0 , \quad (2.15)$$

so that eq. (2.3) becomes,

$$-s \gg -s_1, -s_2 \gg -t_1, -t_2 . \quad (2.16)$$

Then the mass-shell condition (2.4) for the intermediate gluon is

$$-\kappa = \frac{(-s_1)(-s_2)}{-s} , \quad (2.17)$$

where $\kappa = -|p_{4\perp}|^2$.

In eq. (2.14), the Regge trajectory has the perturbative expansion,

$$\alpha(t_i) = \bar{g}^2 \bar{\alpha}^{(1)}(t_i) + \bar{g}^4 \bar{\alpha}^{(2)}(t_i) + \bar{g}^6 \bar{\alpha}^{(3)}(t_i) + \mathcal{O}(\bar{g}^8) , \quad (2.18)$$

with $i = 1, 2$, and with the rescaled coupling

$$\bar{g}^2 = g^2 c_{\Gamma} N . \quad (2.19)$$

In eq. (2.14), the coefficient functions C and the gluon-production vertex V are also expanded in the rescaled coupling,

$$C(p_i, p_j, \tau) = C^{(0)}(p_i, p_j) \left(1 + \sum_{r=1}^{s-1} \bar{g}^{2r} \bar{C}^{(r)}(t_k, \tau) + \mathcal{O}(\bar{g}^{2s}) \right) , \quad (2.20)$$

$$V(q_2, q_1, \kappa, \tau) = V^{(0)}(q_2, q_1) \left(1 + \sum_{r=1}^{s-1} \bar{g}^{2r} \bar{V}^{(r)}(t_1, t_2, \kappa, \tau) + \mathcal{O}(\bar{g}^{2s}) \right) .$$

with $(p_i + p_j)^2 = t_k$ where C and V are real, up to overall complex phases in $C^{(0)}$, eq. (2.8), and $V^{(0)}$, eq. (2.9), induced by the complex-valued helicity bases. Note that because several

transverse scales occur, we prefer to associate the renormalisation scale dependence of the trajectory, coefficient function and gluon-production vertex with the loop coefficients rather than in the rescaled coupling,

$$\begin{aligned}\bar{\alpha}^{(n)}(t_i) &= \left(\frac{\mu^2}{-t_i}\right)^{n\epsilon} \alpha^{(n)}, & \bar{C}^{(n)}(t_k, \tau) &= \left(\frac{\mu^2}{-t_k}\right)^{n\epsilon} C^{(n)}(t_k, \tau), \\ \bar{V}^{(n)}(t_1, t_2, \kappa, \tau) &= \left(\frac{\mu^2}{-\kappa}\right)^{n\epsilon} V^{(n)}(t_1, t_2, \kappa, \tau).\end{aligned}\tag{2.21}$$

The perturbative expansion of eq. (2.14) can be written as

$$m_5 = m_5^{(0)} \left(1 + \bar{g}^2 m_5^{(1)} + \bar{g}^4 m_5^{(2)} + \bar{g}^6 m_5^{(3)} + \mathcal{O}(\bar{g}^8)\right).\tag{2.22}$$

In the expansion of eq. (2.22), the knowledge of the l -loop five-point amplitude in multi-Regge kinematics (2.16), together with the l -loop trajectory $\alpha^{(l)}$ and coefficient function $C^{(l)}$, allows one to derive the gluon-production vertex to the same accuracy. The one-loop coefficient is

$$m_5^{(1)}(\epsilon) = \bar{\alpha}^{(1)}(t_1)L_1 + \bar{\alpha}^{(1)}(t_2)L_2 + \bar{C}^{(1)}(t_1, \tau) + \bar{C}^{(1)}(t_2, \tau) + \bar{V}^{(1)}(t_1, t_2, \kappa, \tau).\tag{2.23}$$

where $L_i = \ln(-s_i/\tau)$ and $i = 1, 2$. The one-loop trajectory is [4],

$$\alpha^{(1)} = \frac{2}{\epsilon},\tag{2.24}$$

and the one-loop coefficient function to all orders in ϵ is given by [5, 17–21]

$$C^{(1)}(t, \tau) = \frac{\psi(1+\epsilon) - 2\psi(-\epsilon) + \psi(1)}{\epsilon} - \frac{1}{\epsilon} \ln \frac{-t}{\tau}.\tag{2.25}$$

Since $\alpha^{(1)}$ and $C^{(1)}(t, \tau)$ are known to all orders in ϵ , we see that the order to which $m_5^{(1)}(\epsilon)$ is known dictates the order to which one may extract $V^{(n)}(t_1, t_2, \kappa, \tau)$.

Similarly the two-loop coefficient of the five-point amplitude is

$$\begin{aligned}m_5^{(2)}(\epsilon) &= \frac{1}{2} \left[m_5^{(1)}(\epsilon)\right]^2 + \bar{\alpha}^{(2)}(t_1)L_1 + \bar{\alpha}^{(2)}(t_2)L_2 + \bar{C}^{(2)}(t_1, \tau) + \bar{V}^{(2)}(t_1, t_2, \kappa, \tau) \\ &+ \bar{C}^{(2)}(t_2, \tau) - \frac{1}{2} \left(\bar{C}^{(1)}(t_1, \tau)\right)^2 - \frac{1}{2} \left(\bar{V}^{(1)}(t_1, t_2, \kappa, \tau)\right)^2 - \frac{1}{2} \left(\bar{C}^{(1)}(t_2, \tau)\right)^2,\end{aligned}\tag{2.26}$$

where $m_5^{(1)}(\epsilon)$, $\bar{C}^{(1)}(t, \tau)$ and $\bar{V}^{(1)}(t_1, t_2, \kappa, \tau)$ must be known through to $\mathcal{O}(\epsilon^2)$. The two-loop trajectory, $\alpha^{(2)}$, is known in full QCD [22–26]. In MSYM, it has been computed through to $\mathcal{O}(\epsilon^0)$ directly [27] and using the maximal transcendentality principle [28], and through to $\mathcal{O}(\epsilon^2)$ directly [6],

$$\alpha^{(2)} = -\frac{2\zeta_2}{\epsilon} - 2\zeta_3 - 8\zeta_4\epsilon + (36\zeta_2\zeta_3 + 82\zeta_5)\epsilon^2 + \mathcal{O}(\epsilon^3).\tag{2.27}$$

The MSYM two-loop coefficient function has been computed through to $\mathcal{O}(\epsilon^2)$ [6],

$$\begin{aligned}
 C^{(2)}(t, \tau) &= \frac{2}{\epsilon^4} + \frac{2}{\epsilon^3} \ln \frac{-t}{\tau} - \left(5\zeta_2 - \frac{1}{2} \ln^2 \frac{-t}{\tau} \right) \frac{1}{\epsilon^2} - \left(\zeta_3 + 2\zeta_2 \ln \frac{-t}{\tau} \right) \frac{1}{\epsilon} \\
 &\quad - \frac{55}{4} \zeta_4 + \left(\zeta_2 \zeta_3 - 41\zeta_5 + \zeta_4 \ln \frac{-t}{\tau} \right) \epsilon \\
 &\quad - \left(\frac{95}{2} \zeta_3^2 + \frac{1695}{8} \zeta_6 + (18\zeta_2 \zeta_3 + 42\zeta_5) \ln \frac{-t}{\tau} \right) \epsilon^2 + \mathcal{O}(\epsilon^3) \\
 &= \frac{1}{2} \left[C^{(1)}(t, \tau) \right]^2 + \frac{\zeta_2}{\epsilon^2} + \left(\zeta_3 + \zeta_2 \ln \frac{-t}{\tau} \right) \frac{1}{\epsilon} \\
 &\quad + \left(\zeta_3 \ln \frac{-t}{\tau} - 19\zeta_4 \right) + \left(4\zeta_4 \ln \frac{-t}{\tau} - 2\zeta_2 \zeta_3 - 39\zeta_5 \right) \epsilon \\
 &\quad - \left(48\zeta_3^2 + \frac{1773}{8} \zeta_6 + (18\zeta_2 \zeta_3 + 41\zeta_5) \ln \frac{-t}{\tau} \right) \epsilon^2 + \mathcal{O}(\epsilon^3). \quad (2.28)
 \end{aligned}$$

Armed with this knowledge together with the two-loop amplitude, $m_5^{(2)}(\epsilon)$, one could extract the two-loop Lipatov vertex. However, as we showed in ref. [7], the Lipatov vertex satisfies its own iterative formula, and one can avoid needing to know $m_5^{(2)}(\epsilon)$.

2.3 The two-loop five-point amplitude and the BDS ansatz

In the normalization of refs. [6, 7], the iterative structure of the two-loop five-point amplitude in the $\mathcal{N} = 4$ super Yang-Mills theory is given by [8, 9]

$$m_5^{(2)}(\epsilon) = \frac{1}{2} \left[m_5^{(1)}(\epsilon) \right]^2 + \frac{2G^2(\epsilon)}{G(2\epsilon)} f^{(2)}(\epsilon) m_5^{(1)}(2\epsilon) + 4Const^{(2)} + \mathcal{O}(\epsilon), \quad (2.29)$$

where $Const^{(2)} = -\zeta_2^2/2$, the $f^{(2)}$ function is

$$f^{(2)}(\epsilon) = -\zeta_2 - \zeta_3 \epsilon - \zeta_4 \epsilon^2, \quad (2.30)$$

and

$$G(\epsilon) = \frac{e^{-\gamma\epsilon} \Gamma(1-2\epsilon)}{\Gamma(1+\epsilon) \Gamma^2(1-\epsilon)} = 1 + \mathcal{O}(\epsilon^2), \quad (2.31)$$

and where the one-loop five-point amplitude, $m_5^{(1)}(\epsilon)$, must be known through to $\mathcal{O}(\epsilon^2)$. In ref. [3], the two-loop five-point amplitude has been shown to fulfil the BDS ansatz by the numeric calculation of $m_5^{(1)}(\epsilon)$ through to $\mathcal{O}(\epsilon^2)$ and of $m_5^{(2)}(\epsilon)$ through to finite terms.

In ref. [6], the iterative structure [8, 9] and the Regge factorisation of the two-loop four-point amplitude have been used to write the two-loop Regge trajectory and coefficient function through to finite terms in terms of the constant $Const^{(2)}$, the function $f^{(2)}$, and of the one-loop coefficient function $C^{(1)}(\epsilon)$,

$$\begin{aligned}
 \alpha^{(2)}(\epsilon) &= 2f^{(2)}(\epsilon) \alpha^{(1)}(2\epsilon) + \mathcal{O}(\epsilon), \\
 C^{(2)}(\epsilon) &= \frac{1}{2} \left[C^{(1)}(\epsilon) \right]^2 + \frac{2G^2(\epsilon)}{G(2\epsilon)} f^{(2)}(\epsilon) C^{(1)}(2\epsilon) + 2Const^{(2)} + \mathcal{O}(\epsilon), \quad (2.32)
 \end{aligned}$$

where the one-loop coefficient function $C^{(1)}(\epsilon)$ is needed through to $\mathcal{O}(\epsilon^2)$, and where we stress only the dependence on the dimensional-regularisation parameter ϵ .

Combining eq. (2.32), the iterative structure of the two-loop five-point amplitude (2.29), and the constant term of the high-energy expansion (2.26), one can find an iteration formula for the two-loop gluon-production vertex [7],

$$V^{(2)}(\epsilon) = \frac{1}{2} \left[V^{(1)}(\epsilon) \right]^2 + \frac{2G^2(\epsilon)}{G(2\epsilon)} f^{(2)}(\epsilon) V^{(1)}(2\epsilon) + \mathcal{O}(\epsilon), \quad (2.33)$$

where the one-loop gluon-production vertex must be known through to $\mathcal{O}(\epsilon^2)$. Note that in order to compute the two-loop gluon-production vertex through to finite terms, it is not needed to know the two-loop five-point amplitude or the two-loop coefficient function explicitly. It suffices to know the one-loop five-point amplitude through to $\mathcal{O}(\epsilon^2)$, from which one can derive the one-loop gluon-production vertex to the same accuracy.

2.4 Analytic continuation of the five-point amplitude to the physical region

We analytically continue the high-energy prescription for the colour-stripped amplitude (2.14) to the physical region, where s, s_1, s_2 are positive and t_1, t_2 are negative. The analytic continuation is performed according to the usual Feynman $+i\epsilon$ prescription, e.g., for $s > 0$,

$$\ln(-s - i\epsilon) = \ln s - i\pi. \quad (2.34)$$

It is easy to see that this is equivalent to the replacements,

$$(-s) \rightarrow e^{-i\pi} s, \quad (-s_1) \rightarrow e^{-i\pi} s_1, \quad (-s_2) \rightarrow e^{-i\pi} s_2, \quad (2.35)$$

In the physical region multi-Regge kinematics require that,

$$s \gg s_1, \quad s_2 \gg -t_1, \quad -t_2. \quad (2.36)$$

Eq. (2.35) implies that eqs. (2.23) and (2.26) are continued by $\ln(-s_j) = \ln(s_j) - i\pi$, for $s_j > 0$ and $j = 1, 2$. The mass-shell condition (2.17) and the analytic continuation (2.35) imply that the transverse scale κ is continued as,

$$(-\kappa) \rightarrow e^{-i\pi} \kappa, \quad (2.37)$$

and the mass-shell condition is reduced to the usual one in the physical region, eq. (2.4). Note that the expansions of eqs. (2.18)–(2.21) are still valid, but because of the analytic continuation on κ , which implies that $\ln(-\kappa) = \ln(\kappa) - i\pi$, for $\kappa > 0$, the gluon-production vertex becomes complex,

$$\bar{V}^{(n)}(t_1, t_2, \kappa, \tau) = \left(\frac{\mu^2}{\kappa} \right)^{n\epsilon} V_{\text{phys}}^{(n)}(t_1, t_2, \kappa, \tau), \quad (2.38)$$

with

$$V_{\text{phys}}^{(n)}(t_1, t_2, \kappa, \tau) = e^{i\pi n\epsilon} V^{(n)}(t_1, t_2, e^{-i\pi}(-\kappa), \tau). \quad (2.39)$$

3 The one-loop five-point amplitude

We may write the one-loop five-point amplitude (1.1) for general kinematics as,

$$m_5^{(1)}(1, 2, 3, 4, 5) = m_{5e}^{(1)}(1, 2, 3, 4, 5) + m_{5o}^{(1)}(1, 2, 3, 4, 5), \quad (3.1)$$

where the parity-even and odd contributions are given to all orders in ϵ by [2, 3],

$$m_{5e}^{(1)}(1, 2, 3, 4, 5) = -\frac{1}{4} 2 G(\epsilon) \sum_{\text{cyclic}} s_{12} s_{23} I_4^{1m}(1, 2, 3, 4, 5, \epsilon), \quad (3.2)$$

$$m_{5o}^{(1)}(1, 2, 3, 4, 5) = -\frac{\epsilon}{2} 2 G(\epsilon) \epsilon_{1234} I_5^{6-2\epsilon}(\epsilon), \quad (3.3)$$

where the cyclicity is over $i = 1, \dots, 5$. Here $I_4^{1m}(1, 2, 3, 4, 5, \epsilon)$ is the one-mass box with the massive leg of virtuality s_{45} , $I_5^{6-2\epsilon}(\epsilon)$ is the pentagon evaluated in $6 - 2\epsilon$ dimensions, the contracted Levi-Civita tensor is $\epsilon_{1234} = \text{tr}[\gamma_5 \not{k}_1 \not{k}_2 \not{k}_3 \not{k}_4]$, and we use the normalization of refs. [6, 7], with $G(\epsilon)$ as in eq. (2.31).

For multi-Regge kinematics (2.16) in the Euclidean region (2.15), the parity-even contribution is, to all orders in ϵ ,

$$\begin{aligned} m_{5e}^{(1)}(1, 2, 3, 4, 5) = & \\ & -\frac{1}{\epsilon^2} \left(\frac{\mu^2}{-\kappa} \right)^\epsilon \Gamma(1 + \epsilon) \Gamma(1 - \epsilon) \\ & + \frac{2}{\epsilon} \left(\frac{\mu^2}{-t_1} \right)^\epsilon (\psi(1) - \psi(-\epsilon)) + \frac{1}{\epsilon} \left(\frac{\mu^2}{-t_2} \right)^\epsilon (2\psi(1) - 3\psi(-\epsilon) + \psi(1 + \epsilon)) \\ & + \frac{1}{\epsilon^2} \left(\frac{\mu^2}{-t_1} \right)^\epsilon {}_2F_1 \left(-\epsilon, 1, 1 - \epsilon; \frac{t_1}{t_2} \right) - \frac{1}{\epsilon(1 + \epsilon)} \left(\frac{\mu^2}{-t_2} \right)^\epsilon \frac{t_1}{t_2} {}_2F_1 \left(1, 1 + \epsilon, 2 + \epsilon; \frac{t_1}{t_2} \right) \\ & + \frac{1}{\epsilon} \left(\frac{\mu^2}{-t_1} \right)^\epsilon \ln \frac{s_1}{\kappa} + \frac{1}{\epsilon} \left(\frac{\mu^2}{-t_2} \right)^\epsilon \ln \frac{s_2}{\kappa} \\ & + \frac{1}{\epsilon} \left(\frac{\mu^2}{-t_1} \right)^\epsilon \ln \frac{s_1}{t_2 - t_1} + \frac{1}{\epsilon} \left(\frac{\mu^2}{-t_2} \right)^\epsilon \ln \frac{s_2}{t_2 - t_1}, \end{aligned} \quad (3.4)$$

for $(-t_2) > (-t_1)$, and

$$\begin{aligned} {}_2F_1(-\epsilon, 1, 1 - \epsilon; z) &= 1 - \sum_{n=1}^{\infty} \text{Li}_n(z) \epsilon^n, \\ {}_2F_1(1, 1 + \epsilon, 2 + \epsilon; z) &= \frac{\text{Li}_1(z)}{z} + \left(\frac{\text{Li}_1(z)}{z} - \frac{\text{Li}_2(z)}{z} \right) \epsilon + \left(\frac{\text{Li}_3(z)}{z} - \frac{\text{Li}_2(z)}{z} \right) \epsilon^2 \\ &\quad + \left(\frac{\text{Li}_3(z)}{z} - \frac{\text{Li}_4(z)}{z} \right) \epsilon^3 + \left(\frac{\text{Li}_5(z)}{z} - \frac{\text{Li}_4(z)}{z} \right) \epsilon^4 + \dots \end{aligned} \quad (3.5)$$

where $\text{Li}_1(z) = -\ln(1 - z)$. The parity-even term for $(-t_1) > (-t_2)$ is obtained by exchanging t_1 and t_2 in eq. (3.4). Eq. (3.4) is manifestly real; it is also symmetric in t_1 and t_2 , although not manifestly. It can be put in a manifestly symmetric form, at the price of introducing imaginary parts, which cancel only after combining all the terms. Eq. (3.4)

agrees through to $\mathcal{O}(\epsilon^0)$ with the $\mathcal{N} = 4$ part of the one-loop five-gluon amplitude in QCD [29] in multi-Regge kinematics [18].

The parity-odd contribution is characterised by the contracted Levi-Civita tensor which can be written as,

$$\epsilon_{1234} = s_{12}s_{34} - s_{13}s_{24} + s_{14}s_{23} - 2\langle 12 \rangle [23] \langle 34 \rangle [41]. \quad (3.6)$$

In multi-Regge kinematics (2.16) this becomes

$$\epsilon_{1234} = (-s) (p_{3\perp} p_{4\perp}^* - p_{4\perp} p_{3\perp}^*). \quad (3.7)$$

Therefore we see that in the high-energy limit, the parity-odd contribution (3.3) is given by

$$m_{5o}^{(1)}(1, 2, 3, 4, 5) = -\epsilon G(\epsilon) (-s) (p_{3\perp} p_{4\perp}^* - p_{4\perp} p_{3\perp}^*) \left(\frac{\mu^2}{-\kappa} \right)^\epsilon \mathcal{P}, \quad (3.8)$$

where the function \mathcal{P} is

$$\mathcal{P} = \begin{cases} \frac{1}{st_2} \mathcal{I}^{(IIa)}(\kappa, t_1, t_2) & \text{for } -\sqrt{\frac{st_1}{s_1 s_2}} + \sqrt{\frac{st_2}{s_1 s_2}} > 1 \text{ and } -t_1 < -t_2, \\ \frac{1}{s_1 s_2} \mathcal{I}^{(I)}(\kappa, t_1, t_2) & \text{for } \sqrt{\frac{st_1}{s_1 s_2}} + \sqrt{\frac{st_2}{s_1 s_2}} < 1. \end{cases} \quad (3.9)$$

To all orders in ϵ , $\mathcal{I}^{(IIa)}(\kappa, t_1, t_2)$ is [1],

$$\begin{aligned} \mathcal{I}^{(IIa)}(\kappa, t_1, t_2) = & -\frac{1}{\epsilon^3} y_2^{-\epsilon} \Gamma(1-2\epsilon) \Gamma(1+\epsilon)^2 F_4\left(1-2\epsilon, 1-\epsilon, 1-\epsilon, 1-\epsilon; -y_1, y_2\right) \\ & + \frac{1}{\epsilon^3} \Gamma(1+\epsilon) \Gamma(1-\epsilon) F_4\left(1, 1-\epsilon, 1-\epsilon, 1+\epsilon; -y_1, y_2\right) \\ & - \frac{1}{\epsilon^2} y_1^\epsilon y_2^{-\epsilon} \left\{ \left[\ln y_1 + \psi(1-\epsilon) - \psi(-\epsilon) \right] F_4\left(1, 1-\epsilon, 1+\epsilon, 1-\epsilon; -y_1, y_2\right) \right. \\ & \quad \left. + \frac{\partial}{\partial \delta} F_{0,2}^{2,1} \left(\begin{matrix} 1+\delta & 1+\delta-\epsilon \\ - & - \end{matrix} \middle| \begin{matrix} 1 & - & - & - \\ 1+\delta & 1-\epsilon & 1+\epsilon+\delta & - \end{matrix} \middle| -y_1, y_2 \right) \Big|_{\delta=0} \right\} \\ & + \frac{1}{\epsilon^2} y_1^\epsilon \left\{ \left[\ln y_1 + \psi(1+\epsilon) - \psi(-\epsilon) \right] F_4\left(1, 1+\epsilon, 1+\epsilon, 1+\epsilon; -y_1, y_2\right) \right. \\ & \quad \left. + \frac{\partial}{\partial \delta} F_{0,2}^{2,1} \left(\begin{matrix} 1+\delta & 1+\delta+\epsilon \\ - & - \end{matrix} \middle| \begin{matrix} 1 & - & - & - \\ 1+\delta & 1+\epsilon & 1+\epsilon+\delta & - \end{matrix} \middle| -y_1, y_2 \right) \Big|_{\delta=0} \right\}, \quad (3.10) \end{aligned}$$

with

$$y_1 = \frac{\kappa}{t_2} \quad \text{and} \quad y_2 = \frac{t_1}{t_2}, \quad (3.11)$$

and where we introduced the Appell function

$$F_4(a, b, c, d; x, y) = \sum_{m=0}^{\infty} \sum_{n=0}^{\infty} \frac{(a)_{m+n} (b)_{m+n}}{(c)_m (d)_n} \frac{x^m}{m!} \frac{y^n}{n!}, \quad (3.12)$$

and the Kampé de Fériet function

$$F_{p',q'}^{p,q} \left(\begin{matrix} \alpha_i | \beta_j \gamma_j \\ \alpha'_k | \beta'_\ell \gamma'_\ell \end{matrix} \middle| x, y \right) = \sum_{m=0}^{\infty} \sum_{n=0}^{\infty} \frac{\prod_i (\alpha_i)_{m+n} \prod_j (\beta_j)_m (\gamma_j)_n}{\prod_k (\alpha'_k)_{m+n} \prod_\ell (\beta'_\ell)_m (\gamma'_\ell)_n} \frac{x^m}{m!} \frac{y^n}{n!}, \quad (3.13)$$

with $1 \leq i \leq p$, $1 \leq j \leq q$, $1 \leq k \leq p'$ and $1 \leq \ell \leq q'$, and $(a)_n$ denote the Pochhammer symbols,

$$(a)_n = \frac{\Gamma(a+n)}{\Gamma(a)}. \quad (3.14)$$

The dash in the definition of the Kampé de Fériet functions in eq. (3.13) indicates that a given index is absent in the definition of the hypergeometric series, e.g.,

$$F_{0,2}^{2,1} \left(\begin{matrix} a & b & | & c & - & - \\ - & - & | & d & e & f \end{matrix} \middle| x_1, x_2 \right) = \sum_{n_1=0}^{\infty} \sum_{n_2=0}^{\infty} \frac{(a)_{n_1+n_2} (b)_{n_1+n_2} (c)_{n_1}}{(d)_{n_1} (e)_{n_2} (f)_{n_1}} \frac{x_1^{n_1}}{n_1!} \frac{x_2^{n_2}}{n_2!}. \quad (3.15)$$

In ref. [1], $\mathcal{I}^{(IIa)}(\kappa, t_1, t_2)$ is given as a Laurent expansion through to $\mathcal{O}(\epsilon)$ in terms of Goncharov's multiple polylogarithms [30, 31].

A few comments are in order: eq. (3.8) starts at $\mathcal{O}(\epsilon)$, because eq. (3.10) is finite: all the poles in ϵ cancel. Furthermore, because of the contracted Levi-Civita tensor (3.6) in eq. (1.1), new momentum structures, other than the ones of eqs. (2.8) and (2.9), occur in $m_5^{(1)}$.

In the region where $\sqrt{\frac{st_1}{s_1s_2}} - \sqrt{\frac{st_2}{s_1s_2}} > 1$ and $(-t_1) > (-t_2)$, which we term *I Ib*, $\mathcal{I}^{(I Ib)}$ is given by [1],

$$\mathcal{I}^{(I Ib)}(\kappa, t_1, t_2) = \frac{t_2}{t_1} \mathcal{I}^{(IIa)}(\kappa, t_2, t_1) \quad (3.16)$$

In eq. (3.9), $\mathcal{I}^{(I)}(\kappa, t_1, t_2)$ can be derived from $\mathcal{I}^{(IIa)}(\kappa, t_1, t_2)$ by means of an analytic continuation, as detailed in ref. [1], where it is also given explicitly to all orders in ϵ , as well as a Laurent expansion through to $\mathcal{O}(\epsilon)$ in terms of Goncharov's multiple polylogarithms.

3.1 Soft limit

As discussed in ref. [1], the limit in which the intermediate gluon becomes soft, $p_4 \rightarrow 0$, and thus $\kappa \rightarrow 0$, $t_1 \rightarrow t$ and $t_2 \rightarrow t$, is realised in the regions *IIa* and *I Ib* of eq. (3.9). Thus,

$$\lim_{p_4 \rightarrow 0} m_{5o}^{(1)}(1, 2, 3, 4, 5) = \epsilon G(\epsilon) \frac{p_{3\perp} p_{4\perp}^* - p_{4\perp} p_{3\perp}^*}{t} \mathcal{I}^{(II)}(\kappa, t). \quad (3.17)$$

$\mathcal{I}^{(II)}(\kappa, t)$ is obtained from eq. (3.10) by taking the limits $t_1 \rightarrow t$ and $t_2 \rightarrow t$. Because $\mathcal{I}^{(II)}(\kappa, t)$ is logarithmic in κ/t , the parity-odd contribution is power suppressed and thus vanishes as $p_4 \rightarrow 0$. Therefore the soft limit of the full one-loop five-point amplitude is given solely by the soft limit of the parity-even contribution,

$$\lim_{p_4 \rightarrow 0} m_5^{(1)}(1, 2, 3, 4, 5) = \frac{2}{\epsilon} \left(\frac{\mu^2}{-t} \right)^\epsilon \left(\psi(1+\epsilon) - 2\psi(-\epsilon) + \psi(1) + \ln \frac{s}{t} \right) - \frac{1}{\epsilon^2} \left(\frac{\mu^2}{-\kappa} \right)^\epsilon \frac{\pi\epsilon}{\sin(\pi\epsilon)}. \quad (3.18)$$

Using eq. (C.7), we see that eq. (3.18) fulfills the soft limit of the one-loop five-point amplitude in multi-Regge kinematics (C.4).

4 The one-loop gluon-production vertex

In order to compute the one-loop gluon-production vertex, we use eq. (2.20) and subtract the one-loop trajectory (2.24) and coefficient function (2.25) from the one-loop five-point amplitude (2.23) and (3.4). Thus, we obtain the gluon-production vertex,

$$\bar{V}^{(1)}(t_1, t_2, \tau, \kappa) = \bar{V}_e^{(1)}(t_1, t_2, \tau, \kappa) + \bar{V}_o^{(1)}(t_1, t_2, \kappa), \quad (4.1)$$

in terms of parity-even and odd contributions,

$$\begin{aligned} \bar{V}_e^{(1)}(t_1, t_2, \tau, \kappa) &= m_{5e}^{(1)}(1, 2, 3, 4, 5) - \bar{\alpha}^{(1)}(t_1)L_1 - \bar{\alpha}^{(1)}(t_2)L_2 - \bar{C}^{(1)}(t_1, \tau) - \bar{C}^{(1)}(t_2, \tau), \\ \bar{V}_o^{(1)}(t_1, t_2, \kappa) &= m_{5o}^{(1)}(1, 2, 3, 4, 5). \end{aligned} \quad (4.2)$$

Because the high-energy coefficient functions and the Regge trajectory are parity-even, the parity-odd part of the one-loop gluon-production vertex is equal to the parity-odd part of the five-point amplitude (3.8), and accordingly does not depend on the factorisation scale τ . Using eq. (2.21), in the unphysical region (2.15) the parity-even contribution is, to all orders in ϵ ,

$$\begin{aligned} V_e^{(1)}(t_1, t_2, \tau, \kappa) &= \\ &= -\frac{1}{\epsilon^2} \Gamma(1 + \epsilon) \Gamma(1 - \epsilon) \\ &+ \left(\frac{\kappa}{t_1}\right)^\epsilon \left(\frac{\psi(1) - \psi(1 + \epsilon)}{\epsilon} + \frac{1}{\epsilon} \ln \frac{-t_1}{\tau} \right) + \left(\frac{\kappa}{t_2}\right)^\epsilon \left(\frac{\psi(1) - \psi(-\epsilon)}{\epsilon} + \frac{1}{\epsilon} \ln \frac{-t_2}{\tau} \right) \\ &+ \frac{1}{\epsilon^2} \left(\frac{\kappa}{t_1}\right)^\epsilon {}_2F_1\left(\epsilon, 1, 1 - \epsilon; \frac{t_1}{t_2}\right) - \frac{1}{\epsilon(1 + \epsilon)} \left(\frac{\kappa}{t_2}\right)^\epsilon \frac{t_1}{t_2} {}_2F_1\left(1, 1 + \epsilon, 2 + \epsilon; \frac{t_1}{t_2}\right) \\ &- \frac{1}{\epsilon} \left[\left(\frac{\kappa}{t_1}\right)^\epsilon + \left(\frac{\kappa}{t_2}\right)^\epsilon \right] \left[\ln \frac{-\kappa}{\tau} + \ln \frac{t_1 - t_2}{\tau} \right]. \end{aligned} \quad (4.3)$$

Eq. (4.3) is valid in the region where $(-t_2) > (-t_1)$. The expression in the region where $(-t_2) < (-t_1)$ can be easily obtained by analytic continuation. Using eqs. (2.21) and (3.8), the parity-odd contribution is, to all orders in ϵ ,

$$V_o^{(1)}(t_1, t_2, \kappa) = -\epsilon G(\epsilon) (-s) (p_{3\perp} p_{4\perp}^* - p_{4\perp} p_{3\perp}^*) \mathcal{P}, \quad (4.4)$$

with \mathcal{P} given by eq. (3.9), which also cancels the apparent dependence on s above.

In the soft limit, $\kappa \rightarrow 0$, the parity-even part of the one-loop gluon-production vertex (4.3) agrees to all orders in ϵ with the soft limit of the corresponding QCD vertex (C.8). As we have seen in section (3.1), the parity-odd part vanishes.

By expanding eq. (4.3) through to $\mathcal{O}(\epsilon^2)$, and labelling the coefficients of the terms of $\mathcal{O}(\epsilon)$ as

$$\begin{aligned}
 \text{VC}_1(t_1, t_2) &= \zeta_3 - \text{Li}_3\left(\frac{t_1}{t_2}\right) \\
 \text{VC}_2(t_1, t_2, \tau) &= \ln\frac{t_1}{t_2} \left(\text{Li}_2\left(\frac{t_1}{t_2}\right) + \zeta_2 \right) \\
 &\quad + \frac{1}{3} \ln^3 \frac{-t_1}{\tau} - \frac{1}{2} \ln^2 \frac{-t_1}{\tau} \ln \frac{-t_2}{\tau} + \frac{1}{6} \ln^3 \frac{-t_2}{\tau} \\
 \text{VC}_3(t_1, t_2, \tau) &= \frac{1}{6} \ln^3 \frac{-t_1}{\tau} \ln \frac{-t_2}{\tau} - \frac{1}{8} \ln^4 \frac{-t_1}{\tau} - \frac{1}{24} \ln^4 \frac{-t_2}{\tau} \\
 &\quad - \frac{1}{2} \left(\ln^2 \frac{-t_1}{\tau} - \ln^2 \frac{-t_2}{\tau} \right) \left(\text{Li}_2\left(\frac{t_1}{t_2}\right) + \zeta_2 \right), \tag{4.5}
 \end{aligned}$$

the even part of the one-loop Lipatov vertex becomes

$$\begin{aligned}
 V_e^{(1)}(t_1, t_2, \tau, \kappa) &= -\frac{1}{\epsilon^2} \Gamma(1+\epsilon)\Gamma(1-\epsilon) + \left[\left(\frac{\kappa}{t_1}\right)^\epsilon + \left(\frac{\kappa}{t_2}\right)^\epsilon \right] \left(-\frac{1}{\epsilon} \ln \frac{-\kappa}{\tau} + \epsilon \text{VC}_1(t_1, t_2) \right) \\
 &\quad + \left(-\frac{1}{2} \ln^2 \frac{t_1}{t_2} + \epsilon \text{VC}_2(t_1, t_2, \tau) \right) \left(\frac{-\kappa}{\tau}\right)^\epsilon + \epsilon^2 \text{VC}_3(t_1, t_2, \tau) + \mathcal{O}(\epsilon^3). \tag{4.6}
 \end{aligned}$$

with the expansion of the first term given in eq. (C.9).

The expansion of eq. (4.4) through to $\mathcal{O}(\epsilon^2)$ is provided by the expansion of the functions $\mathcal{I}^{(IIa)}(\kappa, t_1, t_2)$ and $\mathcal{I}^{(I)}(\kappa, t_1, t_2)$ of eq. (3.9) through to $\mathcal{O}(\epsilon)$ in terms of Goncharov's multiple polylogarithms [1].

4.1 Analytic continuation of the one-loop vertex to the physical region

Using eq. (2.39) and the prescription $\ln(-\kappa) = \ln(\kappa) - i\pi$, for $\kappa > 0$, in the physical region where s, s_1, s_2 are positive and t_1, t_2 are negative, the parity-even part of the one-loop gluon-production vertex (4.3) is

$$\begin{aligned}
 V_{e,\text{phys}}^{(1)}(t_1, t_2, \tau, \kappa) &= \\
 &-\frac{1}{\epsilon^2} e^{i\pi\epsilon} \Gamma(1+\epsilon)\Gamma(1-\epsilon) \\
 &+ \left(\frac{\kappa}{-t_1}\right)^\epsilon \left(\frac{\psi(1) - \psi(1+\epsilon)}{\epsilon} + \frac{1}{\epsilon} \ln \frac{-t_1}{\tau} \right) + \left(\frac{\kappa}{-t_2}\right)^\epsilon \left(\frac{\psi(1) - \psi(-\epsilon)}{\epsilon} + \frac{1}{\epsilon} \ln \frac{-t_2}{\tau} \right) \\
 &+ \frac{1}{\epsilon^2} \left(\frac{\kappa}{-t_1}\right)^\epsilon {}_2F_1\left(\epsilon, 1, 1-\epsilon; \frac{t_1}{t_2}\right) - \frac{1}{\epsilon(1+\epsilon)} \left(\frac{\kappa}{-t_2}\right)^\epsilon \frac{t_1}{t_2} {}_2F_1\left(1, 1+\epsilon, 2+\epsilon; \frac{t_1}{t_2}\right) \\
 &- \frac{1}{\epsilon} \left[\left(\frac{\kappa}{-t_1}\right)^\epsilon + \left(\frac{\kappa}{-t_2}\right)^\epsilon \right] \left[\ln \frac{\kappa}{\tau} - i\pi + \ln \frac{t_1 - t_2}{\tau} \right]. \tag{4.7}
 \end{aligned}$$

Using the identity (C.9) and

$$\pi\epsilon \frac{\cos(\pi\epsilon)}{\sin(\pi\epsilon)} = 1 + \epsilon(\psi(1-\epsilon) - \psi(1+\epsilon)), \tag{4.8}$$

the real part of the parity-even one-loop gluon-production vertex becomes

$$\begin{aligned}
 \text{Re } V_{e,\text{phys}}^{(1)}(t_1, t_2, \tau, \kappa) = & \\
 & - \frac{1 + \epsilon(\psi(1 - \epsilon) - \psi(1 + \epsilon))}{\epsilon^2} \\
 & + \left(\frac{\kappa}{-t_1}\right)^\epsilon \left(\frac{\psi(1) - \psi(1 + \epsilon)}{\epsilon} + \frac{1}{\epsilon} \ln \frac{-t_1}{\tau}\right) + \left(\frac{\kappa}{-t_2}\right)^\epsilon \left(\frac{\psi(1) - \psi(-\epsilon)}{\epsilon} + \frac{1}{\epsilon} \ln \frac{-t_2}{\tau}\right) \\
 & + \frac{1}{\epsilon^2} \left(\frac{\kappa}{-t_1}\right)^\epsilon {}_2F_1\left(\epsilon, 1, 1 - \epsilon; \frac{t_1}{t_2}\right) - \frac{1}{\epsilon(1 + \epsilon)} \left(\frac{\kappa}{-t_2}\right)^\epsilon \frac{t_1}{t_2} {}_2F_1\left(1, 1 + \epsilon, 2 + \epsilon; \frac{t_1}{t_2}\right) \\
 & - \frac{1}{\epsilon} \left[\left(\frac{\kappa}{-t_1}\right)^\epsilon + \left(\frac{\kappa}{-t_2}\right)^\epsilon \right] \left[\ln \frac{\kappa}{\tau} + \ln \frac{t_1 - t_2}{\tau} \right], \tag{4.9}
 \end{aligned}$$

which can be readily expanded in ϵ like in eqs. (4.5) and (4.6).

The imaginary part is given by

$$\text{Im } V_{e,\text{phys}}^{(1)}(t_1, t_2, \tau, \kappa) = \frac{\pi}{\epsilon} \left\{ -1 + \left(\frac{\kappa}{-t_1}\right)^\epsilon + \left(\frac{\kappa}{-t_2}\right)^\epsilon \right\}. \tag{4.10}$$

Taking into account the sign flip of the spin structure (3.7), the analytic continuation of the parity-odd part of the one-loop gluon-production vertex (4.4) is

$$V_{o,\text{phys}}^{(1)}(t_1, t_2, \tau, \kappa) = -\epsilon G(\epsilon) s (p_{3\perp} p_{4\perp}^* - p_{4\perp} p_{3\perp}^*) \mathcal{P}_{\text{phys}}, \tag{4.11}$$

where the function $\mathcal{P}_{\text{phys}}$ is,

$$\mathcal{P}_{\text{phys}} = \begin{cases} \frac{1}{st_2} \mathcal{I}_{\text{phys}}^{(IIa)}(\kappa, t_1, t_2) & \text{for } -\sqrt{\frac{-st_1}{s_1 s_2}} + \sqrt{\frac{-st_2}{s_1 s_2}} > 1 \text{ and } (-t_1) < (-t_2), \\ \frac{1}{s_1 s_2} \mathcal{I}_{\text{phys}}^{(I)}(\kappa, t_1, t_2) & \text{for } \sqrt{\frac{-st_1}{s_1 s_2}} + \sqrt{\frac{-st_2}{s_1 s_2}} < 1. \end{cases} \tag{4.12}$$

The analytic continuation (2.37) implies that the ratios y_1 and y_2 , eq. (3.11), are continued as,

$$(-y_1) \rightarrow e^{-i\pi} y_1, \quad y_2 \rightarrow y_2, \tag{4.13}$$

and the functions $\mathcal{I}_{\text{phys}}^{(I,II)}(\kappa, t_1, t_2)$ are continued according to eq. (2.39). Then eq. (3.10) is continued to,

$$\begin{aligned}
 \mathcal{I}_{\text{phys}}^{(IIa)}(\kappa, t_1, t_2) = & \\
 & -e^{i\pi\epsilon} \frac{1}{\epsilon^3} y_2^{-\epsilon} \Gamma(1 - 2\epsilon) \Gamma(1 + \epsilon)^2 F_4\left(1 - 2\epsilon, 1 - \epsilon, 1 - \epsilon, 1 - \epsilon; -y_1, y_2\right) \\
 & + e^{i\pi\epsilon} \frac{1}{\epsilon^3} \Gamma(1 + \epsilon) \Gamma(1 - \epsilon) F_4\left(1, 1 - \epsilon, 1 - \epsilon, 1 + \epsilon; -y_1, y_2\right) \\
 & - \frac{1}{\epsilon^2} (-y_1)^\epsilon y_2^{-\epsilon} \left\{ \left[\ln(-y_1) - i\pi + \psi(1 - \epsilon) - \psi(-\epsilon) \right] F_4(1, 1 - \epsilon, 1 + \epsilon, 1 - \epsilon; -y_1, y_2) \right. \\
 & \quad \left. + \frac{\partial}{\partial \delta} F_{0,2}^{2,1} \left(\begin{matrix} 1 + \delta & 1 + \delta - \epsilon \\ - & - \end{matrix} \middle| \begin{matrix} 1 & - & - \\ 1 + \delta & 1 - \epsilon & 1 + \epsilon + \delta \end{matrix} \middle| -y_1, y_2 \right) \Big|_{\delta=0} \right\}
 \end{aligned}$$

$$\begin{aligned}
 & + \frac{1}{\epsilon^2} (-y_1)^\epsilon \left\{ [\ln(-y_1) - i\pi + \psi(1+\epsilon) - \psi(-\epsilon)] F_4(1, 1+\epsilon, 1+\epsilon, 1+\epsilon; -y_1, y_2) \right. \\
 & \quad \left. + \frac{\partial}{\partial \delta} F_{0,2}^{2,1} \left(\begin{matrix} 1+\delta & 1+\delta+\epsilon \\ - & - \end{matrix} \middle| \begin{matrix} 1 & - & - & - \\ 1+\delta & 1+\epsilon & 1+\epsilon+\delta & - \end{matrix} \middle| -y_1, y_2 \right) \Big|_{\delta=0} \right\}, \quad (4.14)
 \end{aligned}$$

where the Appell and the Kampé de Fériet functions stay real under the analytic continuation [1]. Like in the Euclidean region in section 3, in eq. (4.14) all the poles in ϵ cancel. Eq. (4.14) may be expanded in ϵ in terms of real \mathcal{M} functions, defined by the double series [1],

$$\mathcal{M}(\vec{i}, \vec{j}, \vec{k}; x_1, x_2) = \sum_{n_1=0}^{\infty} \sum_{n_2=0}^{\infty} \binom{n_1+n_2}{n_1}^2 S_{\vec{i}}(n_1) S_{\vec{j}}(n_2) S_{\vec{k}}(n_1+n_2) x_1^{n_1} x_2^{n_2}, \quad (4.15)$$

where $S_{\vec{i}}(n)$ denote nested harmonic numbers [32]. Eq. (4.14) could also be expanded in terms of Goncharov's multiple polylogarithms, at the price of introducing a complicated and fictitious analytic structure: the Goncharov polylogarithms would occur with several spurious imaginary parts, which ultimately would have to cancel in order to respect the fact that the Appell and the Kampé de Fériet functions are real.

Using the identities (4.8) and (C.9), the real part of the function $I_{\text{phys}}^{(IIa)}(\kappa, t_1, t_2)$ is

$$\begin{aligned}
 \text{Re } \mathcal{I}_{\text{phys}}^{(IIa)}(\kappa, t_1, t_2) = & -y_2^{-\epsilon} \frac{1+\epsilon(\psi(1-\epsilon)-\psi(1+\epsilon))}{\epsilon^3} \frac{\Gamma(1-2\epsilon)\Gamma(1+\epsilon)}{\Gamma(1-\epsilon)} F_4(1-2\epsilon, 1-\epsilon, 1-\epsilon, 1-\epsilon; -y_1, y_2) \\
 & + \frac{1+\epsilon(\psi(1-\epsilon)-\psi(1+\epsilon))}{\epsilon^3} F_4(1, 1-\epsilon, 1-\epsilon, 1+\epsilon; -y_1, y_2) \\
 & - (-y_1)^\epsilon y_2^{-\epsilon} \frac{1}{\epsilon^2} \left\{ [\ln(-y_1) + \psi(1-\epsilon) - \psi(-\epsilon)] F_4(1, 1-\epsilon, 1+\epsilon, 1-\epsilon; -y_1, y_2) \right. \\
 & \quad \left. + \frac{\partial}{\partial \delta} F_{0,2}^{2,1} \left(\begin{matrix} 1+\delta & 1+\delta-\epsilon \\ - & - \end{matrix} \middle| \begin{matrix} 1 & - & - & - \\ 1+\delta & 1-\epsilon & 1+\epsilon+\delta & - \end{matrix} \middle| -y_1, y_2 \right) \Big|_{\delta=0} \right\} \\
 & + (-y_1)^\epsilon \frac{1}{\epsilon^2} \left\{ [\ln(-y_1) + \psi(1+\epsilon) - \psi(-\epsilon)] F_4(1, 1+\epsilon, 1+\epsilon, 1+\epsilon; -y_1, y_2) \right. \\
 & \quad \left. + \frac{\partial}{\partial \delta} F_{0,2}^{2,1} \left(\begin{matrix} 1+\delta & 1+\delta+\epsilon \\ - & - \end{matrix} \middle| \begin{matrix} 1 & - & - & - \\ 1+\delta & 1+\epsilon & 1+\epsilon+\delta & - \end{matrix} \middle| -y_1, y_2 \right) \Big|_{\delta=0} \right\}, \quad (4.16)
 \end{aligned}$$

which, if desired, may be expanded in ϵ in terms of real \mathcal{M} functions.

The imaginary part is

$$\begin{aligned}
 \text{Im } \mathcal{I}_{\text{phys}}^{(IIa)}(\kappa, t_1, t_2) = & \frac{\pi}{\epsilon^2} \left\{ -y_2^{-\epsilon} \frac{\Gamma(1-2\epsilon)\Gamma(1+\epsilon)}{\Gamma(1-\epsilon)} F_4(1-2\epsilon, 1-\epsilon, 1-\epsilon, 1-\epsilon; -y_1, y_2) \right. \\
 & + F_4(1, 1-\epsilon, 1-\epsilon, 1+\epsilon; -y_1, y_2) + (-y_1)^\epsilon y_2^{-\epsilon} F_4(1, 1-\epsilon, 1+\epsilon, 1-\epsilon; -y_1, y_2) \\
 & \left. - (-y_1)^\epsilon F_4(1, 1+\epsilon, 1+\epsilon, 1+\epsilon; -y_1, y_2) \right\}. \quad (4.17)
 \end{aligned}$$

The Appell functions in eq. (4.17) are all reducible to Gauss' hypergeometric function. We find

$$\begin{aligned} \text{Im } \mathcal{I}_{\text{phys}}^{(IIa)}(\kappa, t_1, t_2) &= \frac{\pi}{\epsilon^2} \frac{1}{\sqrt{\lambda(1, -y_1, y_2)}} \left\{ -y_2^{-\epsilon} \frac{\Gamma(1-2\epsilon)\Gamma(1+\epsilon)}{\Gamma(1-\epsilon)} \lambda(1, -y_1, y_2)^\epsilon \right. \\ &\quad + {}_2F_1\left(1, 2\epsilon, 1+\epsilon; \frac{(1-\lambda_1)\lambda_2}{1-\lambda_1\lambda_2}\right) + (-y_1)^\epsilon y_2^{-\epsilon} {}_2F_1\left(1, 2\epsilon, 1+\epsilon; \frac{\lambda_1(1-\lambda_2)}{1-\lambda_1\lambda_2}\right) \\ &\quad \left. - (-y_1)^\epsilon {}_2F_1\left(1, 2\epsilon, 1+\epsilon; \frac{\lambda_1\lambda_2}{1-\lambda_1\lambda_2}\right) \right\}, \end{aligned} \quad (4.18)$$

where λ denotes the Källén function, $\lambda(x, y, z) = x^2 + y^2 + z^2 - 2xy - 2xz - 2yz$, and

$$\begin{aligned} \lambda_1 &= \frac{-1}{2y_1} \left(y_2 - y_1 - 1 + \sqrt{\lambda(1, -y_1, y_2)} \right) \\ \lambda_2 &= \frac{1}{2y_2} \left(y_2 - y_1 - 1 + \sqrt{\lambda(1, -y_1, y_2)} \right). \end{aligned} \quad (4.19)$$

The hypergeometric function can be expanded as a Taylor series in ϵ ,

$${}_2F_1(1, 2\epsilon, 1+\epsilon; z) = 1 - 2\epsilon \ln(1-z) + 2\epsilon^2 \left(\frac{1}{2} \ln^2(1-z) - \text{Li}_2(z) \right) + \mathcal{O}(\epsilon^3). \quad (4.20)$$

5 The two-loop gluon-production vertex

In terms of parity-even and odd contributions, the two-loop gluon-production vertex is

$$V^{(2)}(t_1, t_2, \tau, \kappa) = V_e^{(2)}(t_1, t_2, \tau, \kappa) + V_o^{(2)}(t_1, t_2, \tau, \kappa). \quad (5.1)$$

Using eq. (4.1) and the iteration formula (2.33), eq. (5.1) becomes

$$V_e^{(2)}(\epsilon) = \frac{1}{2} \left[V_e^{(1)}(\epsilon) \right]^2 + \frac{2G^2(\epsilon)}{G(2\epsilon)} f^{(2)}(\epsilon) V_e^{(1)}(2\epsilon) + \mathcal{O}(\epsilon), \quad (5.2)$$

$$V_o^{(2)}(\epsilon) = V_e^{(1)}(\epsilon) V_o^{(1)}(\epsilon) + \mathcal{O}(\epsilon), \quad (5.3)$$

where the parity-even and odd parts of the one-loop gluon-production vertex must be known through to $\mathcal{O}(\epsilon^2)$. We used the fact that $V_o^{(1)}(\epsilon) = \mathcal{O}(\epsilon)$, so it does not contribute to the square of the one-loop vertex in eq. (5.2), and to the term proportional to $f^{(2)}$ in eq. (5.3).

In the unphysical Euclidean region (2.15), eq. (5.2) becomes

$$\begin{aligned} &V_e^{(2)}(t_1, t_2, \tau, \kappa) \\ &= \frac{1}{2\epsilon^4} \left(\frac{\pi\epsilon}{\sin(\pi\epsilon)} \right)^2 - \frac{2G^2(\epsilon)}{G(2\epsilon)} f^{(2)}(\epsilon) \frac{1}{4\epsilon^2} \frac{2\pi\epsilon}{\sin(2\pi\epsilon)} \\ &\quad + \frac{1}{8} \ln^4 \frac{t_1}{t_2} - \text{VC}_3(t_1, t_2, \tau) + \zeta_2 \ln^2 \frac{t_1}{t_2} \\ &\quad + \left[\left(\frac{\kappa}{t_1} \right)^{2\epsilon} + \left(\frac{\kappa}{t_2} \right)^{2\epsilon} \right] \left[\frac{1}{2\epsilon^2} \ln^2 \frac{-\kappa}{\tau} - \left(\frac{1}{\epsilon} f^{(2)}(\epsilon) + \text{VC}_1(t_1, t_2) \right) \ln \frac{-\kappa}{\tau} \right] \end{aligned}$$

$$\begin{aligned}
& + \left(\frac{\kappa}{t_1}\right)^\epsilon \left(\frac{\kappa}{t_2}\right)^\epsilon \left(\frac{1}{\epsilon^2} \ln^2 \frac{-\kappa}{\tau} - 2 \ln \frac{-\kappa}{\tau} \text{VC}_1(t_1, t_2)\right) \\
& - \left[\left(\frac{\kappa}{t_1}\right)^\epsilon + \left(\frac{\kappa}{t_2}\right)^\epsilon\right] \frac{1}{\epsilon^2} \frac{\pi\epsilon}{\sin(\pi\epsilon)} \left(-\frac{1}{\epsilon} \ln \frac{-\kappa}{\tau} + \epsilon \text{VC}_1(t_1, t_2)\right) \\
& - \left[\left(\frac{\kappa}{t_1}\right)^\epsilon + \left(\frac{\kappa}{t_2}\right)^\epsilon\right] \left(\frac{-\kappa}{\tau}\right)^\epsilon \frac{1}{\epsilon} \ln \frac{-\kappa}{\tau} \left(-\frac{1}{2} \ln^2 \frac{t_1}{t_2} + \epsilon \text{VC}_2(t_1, t_2, \tau)\right) \\
& - \left(\frac{-\kappa}{\tau}\right)^\epsilon \frac{1}{\epsilon^2} \frac{\pi\epsilon}{\sin(\pi\epsilon)} \left(-\frac{1}{2} \ln^2 \frac{t_1}{t_2} + \epsilon \text{VC}_2(t_1, t_2, \tau)\right) + \mathcal{O}(\epsilon), \tag{5.4}
\end{aligned}$$

where we have used eq. (4.6) and collected the terms according to the different analytic structures.

The parity-odd part of the two-loop gluon-production vertex, $V_o^{(2)}(t_1, t_2, \tau, \kappa)$, starts at $\mathcal{O}(\epsilon^{-1})$ and is given by the product of eqs. (4.3) and (4.4).

The analytic continuation of the two-loop gluon-production vertex to the physical region where s, s_1, s_2 are positive and t_1, t_2 are negative, may be performed as in section (4.1).

6 Conclusions

In this paper we have computed the one-loop five-point amplitude $m_5^{(1)}$ in the planar $\mathcal{N} = 4$ supersymmetric Yang-Mills theory in multi-Regge kinematics, using the calculation of the one-loop pentagon in $D = 6 - 2\epsilon$ performed in a companion paper [1]. We have presented $m_5^{(1)}$ in the Euclidean region (2.16) as an expression to all orders in ϵ in terms of parity-even, eq. (3.4), and parity-odd contributions, eq. (3.8), starting at $\mathcal{O}(\epsilon^{-2})$ and at $\mathcal{O}(\epsilon)$, respectively.

Using the high-energy factorisation for colour-stripped amplitudes, we have computed the one-loop gluon-production vertex to all orders in ϵ in eqs. (4.3) and (4.4). Because the high-energy coefficient functions and the Regge trajectory are parity-even, the parity-odd part of the one-loop gluon-production vertex equals the parity-odd part of the one-loop five-point amplitude, and thus appears at $\mathcal{O}(\epsilon)$. The Laurent expansion in ϵ through to $\mathcal{O}(\epsilon^2)$ is given in eq. (4.6) for the parity-even part, and in ref. [1] for the parity-odd part in terms of Goncharov’s multiple polylogarithms. In eqs. (4.7) and (4.11), we have continued analytically the all-orders-in- ϵ one-loop gluon-production vertex to the physical region. The even-parity part may be easily expanded in ϵ ; the odd-parity part may be more conveniently expanded in ϵ in terms of real \mathcal{M} functions, as in ref. [1].

The iterative structure of the two-loop five-point amplitude implied by the BDS ansatz, together with the high-energy factorisation, implies an iterative structure of the gluon-production vertex. Thus, the knowledge of the one-loop gluon-production vertex through to $\mathcal{O}(\epsilon^2)$, allows us to perform the first computation of the two-loop gluon-production vertex through to finite terms, which we present in eq. (5.4) as an expansion starting at $\mathcal{O}(\epsilon^{-4})$. The parity-odd part of the two-loop gluon-production vertex appears at $\mathcal{O}(\epsilon^{-1})$ and is given by the product of eqs. (4.3) and (4.4).³

³In ref. [33] the logarithm of the gluon-production vertex has been introduced. If exponentiated, it yields at two-loop order the poles in ϵ through to $\mathcal{O}(\epsilon^{-2})$, but it misses the single poles in ϵ , as well as the finite terms. Accordingly, it lacks completely the parity-odd contribution.

If augmented by the soft-limit contribution to $\mathcal{O}(\epsilon)$, which is as yet unknown, the two-loop gluon-production vertex could be used as one of the building blocks of the kernel of a BFKL equation at next-to-next-to-leading logarithmic (NNLL) accuracy. The other building blocks are the three-loop Regge trajectory [6, 33–35], the one-loop vertex for the emission of two gluons along the ladder (computed in [33] only for two gluons of the same helicity) and the tree vertex for the emission of three gluons along the ladder [36, 37].

Acknowledgments

CD and VDD thank the IPPP Durham and EWNG and CD thank the LNF Frascati for the warm hospitality at various stages of this work. CD is a research fellow of the *Fonds National de la Recherche Scientifique*, Belgium. This work was partly supported by MIUR under contract 2006020509_04, and by the EC Marie-Curie Research Training Network “Tools and Precision Calculations for Physics Discoveries at Colliders” under contract MRTN-CT-2006-035505. EWNG gratefully acknowledges the support of the Wolfson Foundation and the Royal Society.

A Multi-parton kinematics

We consider the production of three gluons of outgoing momentum p_i , with $i = 3, \dots, 5$ in the scattering between two gluons of ingoing momenta p_1 and p_2 .⁴

Using light-cone coordinates $p^\pm = p_0 \pm p_z$, and complex transverse coordinates $p_\perp = p^x + ip^y$, with scalar product $2p \cdot q = p^+q^- + p^-q^+ - p_\perp q_\perp^* - p_\perp^* q_\perp$, the 4-momenta are,

$$\begin{aligned}
 p_2 &= (p_2^+/2, 0, 0, p_2^+/2) \equiv (p_2^+, 0; 0, 0) , \\
 p_1 &= (p_1^-/2, 0, 0, -p_1^-/2) \equiv (0, p_1^-; 0, 0) , \\
 p_i &= ((p_i^+ + p_i^-)/2, \text{Re}[p_{i\perp}], \text{Im}[p_{i\perp}], (p_i^+ - p_i^-)/2) \\
 &\equiv (|p_{i\perp}|e^{y_i}, |p_{i\perp}|e^{-y_i}; |p_{i\perp}| \cos \phi_i, |p_{i\perp}| \sin \phi_i) ,
 \end{aligned}
 \tag{A.1}$$

where y is the rapidity. The first notation above is the standard representation $p^\mu = (p^0, p^x, p^y, p^z)$, while in the second we have the + and - components on the left of the semicolon, and on the right the transverse components. In the following, if not differently stated, p_i and p_j are always understood to lie in the range $3 \leq i, j \leq n$. The mass-shell condition is $|p_{i\perp}|^2 = p_i^+ p_i^-$. Using momentum conservation,

$$0 = \sum_{i=3}^5 p_{i\perp} , \quad p_2^+ = - \sum_{i=3}^5 p_i^+ , \quad p_1^- = - \sum_{i=3}^5 p_i^- ,
 \tag{A.2}$$

the Mandelstam invariants may be written as,

$$s_{ij} = 2p_i \cdot p_j = p_i^+ p_j^- + p_i^- p_j^+ - p_{i\perp} p_{j\perp}^* - p_{i\perp}^* p_{j\perp} ,
 \tag{A.3}$$

⁴By convention we consider the scattering in the unphysical region where all momenta are taken as outgoing, and then we analytically continue to the physical region where $p_1^0 < 0$ and $p_2^0 < 0$.

so that

$$\begin{aligned}
 s &= 2p_1 \cdot p_2 = \sum_{i,j=3}^5 p_i^+ p_j^-, \\
 s_{2i} &= 2p_2 \cdot p_i = -\sum_{j=3}^5 p_i^- p_j^+, \\
 s_{1i} &= 2p_1 \cdot p_i = -\sum_{j=3}^5 p_i^+ p_j^-.
 \end{aligned}
 \tag{A.4}$$

Using the spinor representation of ref. [36],

$$\begin{aligned}
 \psi_+(p_i) &= \begin{pmatrix} \sqrt{p_i^+} \\ \sqrt{p_i^-} e^{i\phi_i} \\ 0 \\ 0 \end{pmatrix}, & \psi_-(p_i) &= \begin{pmatrix} 0 \\ 0 \\ \sqrt{p_i^-} e^{-i\phi_i} \\ -\sqrt{p_i^+} \end{pmatrix}, \\
 \psi_+(p_2) &= i \begin{pmatrix} \sqrt{-p_2^+} \\ 0 \\ 0 \\ 0 \end{pmatrix}, & \psi_-(p_2) &= i \begin{pmatrix} 0 \\ 0 \\ 0 \\ -\sqrt{-p_2^+} \end{pmatrix}, \\
 \psi_+(p_1) &= -i \begin{pmatrix} 0 \\ \sqrt{-p_1^-} \\ 0 \\ 0 \end{pmatrix}, & \psi_-(p_1) &= -i \begin{pmatrix} 0 \\ 0 \\ \sqrt{-p_1^-} \\ 0 \end{pmatrix}.
 \end{aligned}
 \tag{A.5}$$

for the momenta (A.1),⁵ the spinor products are

$$\begin{aligned}
 \langle 21 \rangle &= -\sqrt{s}, \\
 \langle 2i \rangle &= -i \sqrt{\frac{-p_2^+}{p_i^+}} p_{i\perp}, \\
 \langle i1 \rangle &= i \sqrt{-p_1^- p_i^+}, \\
 \langle ij \rangle &= p_{i\perp} \sqrt{\frac{p_j^+}{p_i^+}} - p_{j\perp} \sqrt{\frac{p_i^+}{p_j^+}},
 \end{aligned}
 \tag{A.6}$$

where we have used the mass-shell condition $|p_{i\perp}|^2 = p_i^+ p_i^-$.

⁵The spinors of the incoming partons must be continued to negative energy after the complex conjugation, e.g. $\overline{\psi_+(p_2)} = i \left(\sqrt{-p_2^+}, 0, 0, 0 \right)$.

B Multi-Regge kinematics

In multi-Regge kinematics, we require that the gluons are strongly ordered in rapidity and have comparable transverse momentum (2.1). This is equivalent to requiring a strong ordering of the light-cone coordinates,

$$p_3^+ \gg p_4^+ \gg p_5^+; \quad p_3^- \ll p_4^- \ll p_5^-. \quad (\text{B.1})$$

Momentum conservation (A.2) then becomes

$$0 = \sum_{i=3}^5 p_{i\perp}, \quad p_2^+ \simeq -p_3^+, \quad p_1^- \simeq -p_5^-, \quad (\text{B.2})$$

where the \simeq sign is understood to mean “equals up to corrections of next-to-leading accuracy”. The Mandelstam invariants (A.4) are reduced to,

$$\begin{aligned} s &= 2p_1 \cdot p_2 \simeq p_3^+ p_5^-, \\ s_{2i} &= 2p_2 \cdot p_i \simeq -p_3^+ p_i^-, \\ s_{1i} &= 2p_1 \cdot p_i \simeq -p_i^+ p_5^-, \\ s_{ij} &= 2p_i \cdot p_j \simeq p_i^+ p_j^- \quad i < j. \end{aligned} \quad (\text{B.3})$$

The product of the two successive invariants s_{34} and s_{45} fixes the mass shell of gluon 4,

$$s_{34}s_{45} \simeq p_3^+ p_4^- p_4^+ p_5^- = |p_{4\perp}|^2 p_3^+ p_5^- \simeq |p_{4\perp}|^2 s.$$

Thus,

$$|p_{4\perp}|^2 = \frac{s_{34}s_{45}}{s}. \quad (\text{B.4})$$

The spinor products (A.6) are,

$$\begin{aligned} \langle 21 \rangle &\simeq -\sqrt{p_3^+ p_5^-}, \\ \langle 2i \rangle &\simeq -i \sqrt{\frac{p_3^+}{p_i^+}} p_{i\perp}, \\ \langle i1 \rangle &\simeq i \sqrt{p_i^+ p_5^-}, \\ \langle ij \rangle &\simeq -\sqrt{\frac{p_i^+}{p_j^+}} p_{j\perp} \quad \text{for } y_i > y_j. \end{aligned} \quad (\text{B.5})$$

C The soft limit of the one-loop five-point amplitude

We consider the five-point amplitude of section 2.2, and take the limit where the intermediate gluon becomes soft, $p_4 \rightarrow 0$. In this limit, the one-loop five-point amplitude factorises as [19, 38],

$$\begin{aligned} \lim_{p_4 \rightarrow 0} m_5^{1\text{-loop}}(1, 2, 3, 4^\lambda, 5) &= \text{Soft}^{\text{tree}}(3, 4^\lambda, 5) m_4^{1\text{-loop}}(1, 2, 3, 5) \\ &\quad + \text{Soft}^{1\text{-loop}}(3, 4^\lambda, 5) m_4^{\text{tree}}(1, 2, 3, 5) \end{aligned} \quad (\text{C.1})$$

where the one-loop soft-gluon function, to all orders of ϵ , is

$$\text{Soft}^{1\text{-loop}}(3, 4^\lambda, 5) = -\bar{g}^2 \frac{1}{\epsilon^2} \frac{\pi\epsilon}{\sin(\pi\epsilon)} \left(\frac{\mu^2(-s_{35})}{(-s_{34})(-s_{45})} \right)^\epsilon \text{Soft}^{\text{tree}}(3, 4^\lambda, 5) \quad (\text{C.2})$$

and the tree-level soft function is

$$\text{Soft}^{\text{tree}}(3, 4^+, 5) = \frac{\langle 35 \rangle}{\langle 34 \rangle \langle 45 \rangle}. \quad (\text{C.3})$$

For the MHV amplitude we are considering, the soft limit for a negative helicity gluon is trivial and is obtained from this by helicity reversal. In multi-Regge kinematics (2.16), $s_{35} = s$; then, using the on-shell condition (2.17) and the normalisation of eq. (2.22), the soft-gluon limit of the one-loop five-point coefficient becomes

$$\lim_{p_4 \rightarrow 0} m_5^{(1)}(1, 2, 3, 4, 5) = m_4^{(1)}(1, 2, 3, 5) - \frac{1}{\epsilon^2} \frac{\pi\epsilon}{\sin(\pi\epsilon)} \left(\frac{\mu^2}{-\kappa} \right)^\epsilon, \quad (\text{C.4})$$

where we have factored out

$$\lim_{p_4 \rightarrow 0} m_5^{(0)}(1, 2, 3, 4^\lambda, 5) = m_4^{(0)}(1, 2, 3, 5) \text{Soft}^{\text{tree}}(3, 4^\lambda, 5). \quad (\text{C.5})$$

In addition, in the soft limit of gluon 4, we can write the one-loop coefficient (2.23) as,

$$\lim_{\kappa \rightarrow 0} m_5^{(1)}(1, 2, 3, 4, 5) = m_4^{(1)}(1, 2, 3, 5) + \bar{\alpha}^{(1)}(t) \ln \frac{-\kappa}{\tau} + \lim_{\kappa \rightarrow 0} \bar{V}^{(1)}(t, t, \tau, \kappa), \quad (\text{C.6})$$

with $t_1 = t_2 = t$ and

$$m_4^{(1)} = \bar{\alpha}^{(1)}(t) \ln \frac{-s}{\tau} + 2\bar{C}^{(1)}(t, \tau). \quad (\text{C.7})$$

Equating eqs. (C.4) and (C.6) and using eqs. (2.21) and (2.24), we obtain the soft limit of the one-loop gluon-production vertex, to all orders of ϵ [18],

$$\lim_{\kappa \rightarrow 0} V^{(1)}(t, t, \tau, \kappa) = -\frac{1}{\epsilon^2} \frac{\pi\epsilon}{\sin(\pi\epsilon)} - \frac{2}{\epsilon} \left(\frac{\kappa}{t} \right)^\epsilon \ln \frac{-\kappa}{\tau}, \quad (\text{C.8})$$

with

$$\begin{aligned} \frac{\pi\epsilon}{\sin(\pi\epsilon)} &= \Gamma(1 + \epsilon)\Gamma(1 - \epsilon) = 1 + \zeta_2\epsilon^2 + \frac{7}{4}\zeta_4\epsilon^4 + \frac{31}{16}\zeta_6\epsilon^6 + \dots \\ &= \sum_{n=0}^{\infty} c_n \epsilon^{2n}, \quad \text{with } c_0 = 1, \quad c_n = \frac{2^{2n-1} - 1}{2^{2(n-1)}} \zeta_{2n}. \end{aligned} \quad (\text{C.9})$$

References

- [1] V. Del Duca, C. Duhr, E.W. Nigel Glover and V.A. Smirnov, *The one-loop pentagon to higher orders in epsilon*, [arXiv:0905.0097](#) [SPIRES].
- [2] Z. Bern, L.J. Dixon, D.C. Dunbar and D.A. Kosower, *One-loop self-dual and $N = 4$ super Yang-Mills*, *Phys. Lett. B* **394** (1997) 105 [[hep-th/9611127](#)] [SPIRES].

- [3] Z. Bern, M. Czakon, D.A. Kosower, R. Roiban and V.A. Smirnov, *Two-loop iteration of five-point $N = 4$ super-Yang-Mills amplitudes*, *Phys. Rev. Lett.* **97** (2006) 181601 [[hep-th/0604074](#)] [[SPIRES](#)].
- [4] E.A. Kuraev, L.N. Lipatov and V.S. Fadin, *Multi-Reggeon processes in the Yang-Mills theory*, *Sov. Phys. JETP* **44** (1976) 443 [[SPIRES](#)].
- [5] V.S. Fadin and L.N. Lipatov, *Radiative corrections to QCD scattering amplitudes in a multi-Regge kinematics*, *Nucl. Phys.* **B 406** (1993) 259 [[SPIRES](#)].
- [6] V. Del Duca and E.W.N. Glover, *Testing high-energy factorization beyond the next-to-leading-logarithmic accuracy*, *JHEP* **05** (2008) 056 [[arXiv:0802.4445](#)] [[SPIRES](#)].
- [7] V. Del Duca, C. Duhr and E.W.N. Glover, *Iterated amplitudes in the high-energy limit*, *JHEP* **12** (2008) 097 [[arXiv:0809.1822](#)] [[SPIRES](#)].
- [8] C. Anastasiou, Z. Bern, L.J. Dixon and D.A. Kosower, *Planar amplitudes in maximally supersymmetric Yang-Mills theory*, *Phys. Rev. Lett.* **91** (2003) 251602 [[hep-th/0309040](#)] [[SPIRES](#)].
- [9] Z. Bern, L.J. Dixon and V.A. Smirnov, *Iteration of planar amplitudes in maximally supersymmetric Yang-Mills theory at three loops and beyond*, *Phys. Rev.* **D 72** (2005) 085001 [[hep-th/0505205](#)] [[SPIRES](#)].
- [10] M.L. Mangano and S.J. Parke, *Multi-parton amplitudes in gauge theories*, *Phys. Rept.* **200** (1991) 301 [[hep-th/0509223](#)] [[SPIRES](#)].
- [11] V. Del Duca, *Parke-Taylor amplitudes in the multi-Regge kinematics*, *Phys. Rev.* **D 48** (1993) 5133 [[hep-ph/9304259](#)] [[SPIRES](#)].
- [12] V. Del Duca, *Equivalence of the Parke-Taylor and the Fadin-Kuraev-Lipatov amplitudes in the high-energy limit*, *Phys. Rev.* **D 52** (1995) 1527 [[hep-ph/9503340](#)] [[SPIRES](#)].
- [13] V. Del Duca, L.J. Dixon and F. Maltoni, *New color decompositions for gauge amplitudes at tree and loop level*, *Nucl. Phys.* **B 571** (2000) 51 [[hep-ph/9910563](#)] [[SPIRES](#)].
- [14] V. Del Duca, *Next-to-leading corrections to the BFKL equation*, [hep-ph/9605404](#) [[SPIRES](#)].
- [15] L.N. Lipatov, *Reggeization of the vector meson and the vacuum singularity in nonabelian gauge theories*, *Sov. J. Nucl. Phys.* **23** (1976) 338 [[SPIRES](#)].
- [16] L.N. Lipatov, *High-energy scattering in QCD and in quantum gravity and two-dimensional field theories*, *Nucl. Phys.* **B 365** (1991) 614 [[SPIRES](#)].
- [17] V. Del Duca and C.R. Schmidt, *Virtual next-to-leading corrections to the impact factors in the high-energy limit*, *Phys. Rev.* **D 57** (1998) 4069 [[hep-ph/9711309](#)] [[SPIRES](#)].
- [18] V. Del Duca and C.R. Schmidt, *Virtual next-to-leading corrections to the Lipatov vertex*, *Phys. Rev.* **D 59** (1999) 074004 [[hep-ph/9810215](#)] [[SPIRES](#)].
- [19] Z. Bern, V. Del Duca and C.R. Schmidt, *The infrared behavior of one-loop gluon amplitudes at next-to-next-to-leading order*, *Phys. Lett.* **B 445** (1998) 168 [[hep-ph/9810409](#)] [[SPIRES](#)].
- [20] V.S. Fadin and R. Fiore, *Quark contribution to the gluon-gluon-Reggeon vertex in QCD*, *Phys. Lett.* **B 294** (1992) 286 [[SPIRES](#)].
- [21] V.S. Fadin, R. Fiore and A. Quartarolo, *Radiative corrections to quark quark Reggeon vertex in QCD*, *Phys. Rev.* **D 50** (1994) 2265 [[hep-ph/9310252](#)] [[SPIRES](#)].

- [22] V.S. Fadin, M.I. Kotsky and R. Fiore, *Gluon Reggeization in QCD in the next-to-leading order*, *Phys. Lett. B* **359** (1995) 181 [SPIRES].
- [23] V.S. Fadin, R. Fiore and A. Quartarolo, *Reggeization of quark quark scattering amplitude in QCD*, *Phys. Rev. D* **53** (1996) 2729 [hep-ph/9506432] [SPIRES].
- [24] V.S. Fadin, R. Fiore and M.I. Kotsky, *Gluon Regge trajectory in the two-loop approximation*, *Phys. Lett. B* **387** (1996) 593 [hep-ph/9605357] [SPIRES].
- [25] J. Blumlein, V. Ravindran and W.L. van Neerven, *On the gluon Regge trajectory in $O(\alpha_s^2)$* , *Phys. Rev. D* **58** (1998) 091502 [hep-ph/9806357] [SPIRES].
- [26] V. Del Duca and E.W.N. Glover, *The high energy limit of QCD at two loops*, *JHEP* **10** (2001) 035 [hep-ph/0109028] [SPIRES].
- [27] A.V. Kotikov and L.N. Lipatov, *NLO corrections to the BFKL equation in QCD and in supersymmetric gauge theories*, *Nucl. Phys. B* **582** (2000) 19 [hep-ph/0004008] [SPIRES].
- [28] A.V. Kotikov and L.N. Lipatov, *DGLAP and BFKL evolution equations in the $N = 4$ supersymmetric gauge theory*, *Nucl. Phys. B* **661** (2003) 19 [Erratum *ibid.* **B 685** (2004) 405] [hep-ph/0208220] [SPIRES].
- [29] Z. Bern, L.J. Dixon and D.A. Kosower, *One loop corrections to five gluon amplitudes*, *Phys. Rev. Lett.* **70** (1993) 2677 [hep-ph/9302280] [SPIRES].
- [30] A.B. Goncharov, *Multiple polylogarithms, cyclotomy and modular complexes*, *Math. Res. Let.* **5** (1998) 497.
- [31] J. Vollinga and S. Weinzierl, *Numerical evaluation of multiple polylogarithms*, *Comput. Phys. Commun.* **167** (2005) 177 [hep-ph/0410259] [SPIRES].
- [32] J.A.M. Vermaseren, *Harmonic sums, Mellin transforms and integrals*, *Int. J. Mod. Phys. A* **14** (1999) 2037 [hep-ph/9806280] [SPIRES].
- [33] J. Bartels, L.N. Lipatov and A. Sabio Vera, *BFKL pomeron, Reggeized gluons and Bern-Dixon-Smirnov amplitudes*, *Phys. Rev. D* **80** (2009) 045002 [arXiv:0802.2065] [SPIRES].
- [34] J.M. Drummond, G.P. Korchemsky and E. Sokatchev, *Conformal properties of four-gluon planar amplitudes and Wilson loops*, *Nucl. Phys. B* **795** (2008) 385 [arXiv:0707.0243] [SPIRES].
- [35] S.G. Naculich and H.J. Schnitzer, *Regge behavior of gluon scattering amplitudes in $N = 4$ SYM theory*, *Nucl. Phys. B* **794** (2008) 189 [arXiv:0708.3069] [SPIRES].
- [36] V. Del Duca, A. Frizzo and F. Maltoni, *Factorization of tree QCD amplitudes in the high-energy limit and in the collinear limit*, *Nucl. Phys. B* **568** (2000) 211 [hep-ph/9909464] [SPIRES].
- [37] E.N. Antonov, L.N. Lipatov, E.A. Kuraev and I.O. Cherednikov, *Feynman rules for effective Regge action*, *Nucl. Phys. B* **721** (2005) 111 [hep-ph/0411185] [SPIRES].
- [38] D.A. Kosower and P. Uwer, *One-loop splitting amplitudes in gauge theory*, *Nucl. Phys. B* **563** (1999) 477 [hep-ph/9903515] [SPIRES].